

SUCROSE PECTIN INTERACTION FROM SOLUTION TO GELS

Donatella Bulone, Daniela Giacomazza, Mauro Manno, Vincenzo Martorana and Pier Luigi San Biagio

National Research Council-Institute of Biophysics

Via U. La Malfa, 153 I90146 Palermo (ITALY)

ABSTRACT

Pectin is a very important polysaccharide in food technology, due to its ability to thicken or gel in aqueous solution under specific conditions. One of the most common uses of pectin is in making jellies or jams, which requires the addition of a large amount of sucrose to acidic solutions. The role of sucrose in promoting pectin gelation has been ascribed to the strengthening of hydrophobic interactions consistently with its well-known stabilizing effect on protein structure. On the other hand, more specific effects on dimension and stiffness of pectin chains have been suggested by computational work. Here we present measurements of rheology, static and dynamic light scattering on samples of pectin containing different amounts of sucrose, ranging from few percent up to close to the solubility limit of sucrose. This corresponds to spanning from low viscous liquid samples to strong gels. Results show that below the threshold value of 55% w/w, sucrose acts as a critical parameter for the sol/gel transition by increasing the strength of excluded volume and hydrodynamic interactions between polymer chains. A further increase of sucrose above the critical concentration yields gels with a higher viscoelastic component corresponding to a higher amount of frozen structural inhomogeneities.

INTRODUCTION

Understanding the chemical and physical principles of food making is a fascinating task from many different points of view. Indeed, besides the reward of enlightening the cause-effect

relationships implied in many tricks of the art of cooking, it is also an exciting challenge to deal with systems that are among the most complex to be studied. A new interesting perspective in studying such systems is offered by a modern approach based on concepts from soft matter and colloid physics [1,2].

Here we discuss the case of jam or jelly making by using pectin, a natural polysaccharide obtained from citrus peel or apple pomace. Homemade jam or jelly recipes have one to dissolve the pectin powder in hot water with a large amount of sucrose and added lemon juice, and let the solution cool to room or lower temperature until a firm clear gel is formed. With the aim of tracing the gelation mechanism of this system on a chemical physics ground, it is worthwhile considering what is known about the ingredients involved. Pectin is mostly made of a linear chain of α -(1-4)-linked D-galacturonic acid with some of the carboxyl groups esterified with methanol. In some regions of the regular polygalacturonate backbone, the presence of 1-2 linked L-rhamnose residues increases the structural flexibility and provides sites for the attachment of some neutral sugar chains [3]. Depending on the proportion of methyl ester groups, pectin is classified as high methoxyl (HM) having 50% or higher esterification degree, or low methoxyl (LM). Both types of pectin form gels at concentrations of a few grams per liter, but under different conditions: the gelation of LM pectin requires the presence of calcium ions that bind the carboxyl groups of different chains according to the so-called “egg-box” model [4]; HM pectin, which is the type most used in jam or jelly making, forms gels at acid pH (lower than 3.5) only in the presence of a large amount of sugar or similar cosolutes [5-7] which are known to reduce water activity [7-9]. HM pectin has other applications in food industry as a thickening agent or stabilizer.

Sucrose is one of the most common additives in food sweetening or preservation. It is well known that sucrose, like other simple sugars, stabilizes globular proteins against thermal denaturation [10]. The mechanism of this effect has been explained in terms of “preferential hydration” [11], that is a non-homogeneous distribution of the components of a mixed solvent around the macromolecular surface. The preferential hydration results from the balance between the excluded volume effect, due to the different sizes of the two solvent components, and the free energy change associated with the transfer of the macromolecule from pure to mixed solvent [11]. According to the preferential hydration model, sucrose falls in the category of preferentially excluded cosolutes. In fact, the model can explain much experimental data on sucrose effects on protein functionality, but it fails in some cases where there is a tendency to favor the exposure of hydrophobic surfaces [12,13] that could be attributed to a direct interaction between sucrose and protein. Sucrose’s effects on protein gel formation are too complex to be explained by a single mechanism. Protein gels are formed only upon protein unfolding; an increase of the gelation

temperature at increasing sucrose concentration is commonly observed [12-17] due to an increase in thermal stability. What remains puzzling is the non-monotonic behavior of the gelation rate and gel strength on varying sucrose concentration. The competition between the reinforcement of molecular interactions and the viscosity increase that could hinder molecular encounters, has been proposed as a possible explanation [13, 15-17].

Even more controversial are the opinions about the effect of sucrose and other sugars on the gelation of biopolymers. Similar to the case of proteins gels, a different behavior is observed at relatively low or high sugar concentration. Starting from very low values and increasing sugar concentration up to about 40%, an increase in the gel strength and melting temperature is commonly observed [18-20]. Further addition of sugar causes an abrupt decrease in the elastic modulus in several biopolymeric systems except for case of gelatin [20]. Finally, a fast growth of both elastic and loss modulus is observed on entering the higher concentration region where a rubbery-glass transition occurs [21]. The gel structure at high sugar content is also matter of controversy, since the gel network has been alternately described as made of aggregated particles [22] or flexible and extended chains, lightly cross-linked [23]. In this scenario the sucrose (and more generally sugars) may play different roles through modulation of the hydrophobic interaction, direct binding to polymeric chains, or bulk viscosity increase. It has been recently shown that the gelation behaviour of a high sugar/polymer system can also dramatically depend on the type of sugar added [24], thus showing that no general rules can be easily drawn.

The gelation kinetics of HM pectin with 60% sucrose at different temperatures has been studied by rheology experiments [25]. A non-monotonic dependence of the gelation rate on temperature, with a maximum rate at about 30 °C, was observed and attributed to the different temperature dependence of hydrogen bonding and hydrophobic interactions, both responsible for gelation. Rheological studies at different temperatures on gelled samples with high sugar content have shown that the system has a mechanical response with frequency increase that is typical of a rubbery-glass transition [26-27].

Here we present data on pectin at 0.2 % concentration in sucrose-aqueous solution and gel, spanning a range of sucrose concentration from a few percent up to well above the minimum value (55% w/w) required for observing gel formation at room temperature. We do not present data on gelation kinetics, but simply change the sucrose concentration and study the system, both in sol and gel state, by Light Scattering and Rheology measurements. Light Scattering results on the liquid side had been the subject of our previous work [28] and are here briefly summarized with the intent of providing a more complete description of the system. Data on gelled samples from Dynamic Light Scattering are analyzed in terms of Mode Coupling Theory (MCT), originally developed [29-

31] to describe the dynamical properties of supercooled liquids on approaching the glass transition. A brief account of MCT applications to the description of gelling colloidal systems is given in the “Theory” section.

MATERIALS AND METHODS

Pectin Samples. Slow-set high methoxyl pectin (esterification degree 64.5%) was a kind gift from Hercules Inc. (Wilmington, DE). Water was Millipore Super Q filtered with 0.22 μm filters. All other chemical compounds used were analytical grade from Merck Co. A stock solution at a pectin concentration of 2%w/w was preliminarily prepared by dissolving the powder in pure water at 100 °C for few minutes in a high-speed mixer. The solution was then cooled at room temperature overnight, stored at 4 °C, and used up to 2 or 3 days. Samples at a pectin concentration of 0.2% and different sucrose concentrations were prepared by heating to 100 °C while stirring the potassium citrate buffer (pH 3.4) with the appropriate amount of water and sucrose. Stock pectin solution was then added and boiled for few minutes. The final buffer concentration was 12 mM. Finally, a few microliters of 50% acid citric solution was added to adjust the pH value to 3.1, and samples were filtered at 80 °C through 0.45 μm Corning filters directly into quartz cuvettes. A duplicate of each sample, but without pectin, was prepared by the same procedure to be used for the solvent scattering measurement. Samples at sucrose concentrations of 55% or higher were prepared and divided in several aliquots in glass tubes. One aliquot was put in a quartz cuvette. All the aliquots were put in a thermostated bath at 20 °C. The falling balls method was used to check the samples over time until they were found to be capable of sustaining the ball weight (70 mg).

Static and Dynamic Light Scattering Experiments. Samples that do not form a gel, were allowed to equilibrate at 20 °C for 1 h in the thermostated cell compartment of a Brookhaven Instruments BI200-SM goniometer. The temperature was controlled to within 0.1 °C using a thermostated recirculating bath. The light scattered intensity and time autocorrelation function were measured by using a Brookhaven BI-9000 correlator and a 100 mW Ar laser (Melles Griot) tuned at 514.5 nm or a 35 mW He-Ne laser (Melles Griot) tuned at $\lambda = 632.8$ nm. Measurements were taken at different scattering vectors $q = 4\pi n \lambda_0^{-1} \sin(\theta/2)$ where n is the refraction index of the solution, λ_0 is the wavelength of the incident light, and θ is the scattering angle. Values of the refractive index at different sucrose concentrations were measured by an Abbe refractometer and found almost equal to those of the corresponding sucrose-water solutions [32].

A particular procedure was followed for measurements on gelled samples. Indeed, gels are known to exhibit a nonergodic behavior [33], i.e. the intensity autocorrelation function obtained by

time-averaging is different from that of the ensemble average. This effect arises from the presence of frozen structures that are unable to relax over the experimental time scale. The ensemble-average correlation function was obtained as a collection of more than 100 time-averaged measurements each lasting 10 minutes and taken at different positions by using a motor-driven cell holder. The total was normalized for the total number of detected photons and the number of individual measurements.

Rheological Experiments. Rheological measurements under low amplitude oscillatory shear were performed on a controlled stress AR-1000 rheometer (TA Instruments, UK) using a standard-size double concentric aluminium cylinder (rotor outer radius 21.96 mm, rotor inner radius 20.38 mm, stator outer radius 20.00 mm, cylinder immersed height 59.50 mm, gap 500 μ m). The filtered hot solution was loaded into the cylinder set at 20 $^{\circ}$ C. The cylinder–cylinder upper gap was coated with silicone oil to prevent the evaporation.

Viscosity measurements on liquid samples were performed by applying a shear stress ramp ranging from 0 to 80 Pa and recording the corresponding values of shear strain rate. Viscosity was obtained as the slope of the shear stress-shear strain rate graphs. Three measurements were done for each sample.

Gelling solutions were loaded and left to form the gel. The viscoelastic spectra were measured in a frequency range of 0.02-30 Hz at a strain of 4×10^{-3} , well within the linear viscoelastic region.

THEORY

The Mode Coupling Theory describes the dynamics of a system close to its glass transition limit, through the inclusion in the equations of motion of non-linear delayed interactions (or coupling) between density fluctuations occurring over different lengthscale [29-31]. On varying the parameters that control the static properties, the strength of the dynamic coupling increases with a consequent slowing down of the system dynamics, until a critical value is reached. At this point a dynamic arrest occurs without any change in the structural properties. Close to the critical point, φ_c , the dynamics is governed by the separation parameter:

$$\sigma = k(\varphi - \varphi_c) / \varphi_c \quad (1)$$

Two structural relaxation times with diverging time scales are observed: one, called α -relaxation, is relative to the macroscopic scale and becomes completely arrested at the glass transition point; the other one, called β -relaxation, is relative to the rattling motion of particles confined in cages formed

by the neighbor molecules and persists on traversing the critical point. Over the range of the β -relaxation time scale, intermediate between those corresponding to microscopic motion and long-time α -relaxation, the correlation function of density fluctuations is factorizable and takes the general form:

$$f(q, \tau) = f_c(q) + h(q)c_\sigma g_\pm(\tau/\tau_\beta) \quad (2)$$

where the “ \pm ” refers to a positive or negative σ value, $f_c(q)$ is the nonergodicity parameter, that is the contribution of the frozen structure, $h(q)c_\sigma$ is the amplitude of the fluctuating part, with $c_\sigma = c_0/\sigma^{1/2}$ (c_0 is a system-dependent constant). The temporal dependence is all contained in $g_\pm(\tau/\tau_\beta)$ with $\tau_\beta = t_0/\sigma^\delta$, $\delta = 1/(2a)$ where a is a critical exponent. Two limiting forms of g_\pm are:

$$\text{for } \tau \ll \tau_\beta \quad g_\pm = (\tau/\tau_\beta)^a \quad (4)$$

$$\text{for } \tau_\beta \ll \tau \ll \tau_\alpha \quad g_- = -B(\tau/\tau_\beta)^b \quad (5)$$

The α -relaxation, occurring only on the liquid side, is described by :

$$f(q, \tau) = f_c(q)G(q, \tau/\tau_\alpha) \quad (6)$$

with $\tau_\alpha = t_0/\sigma^{-\gamma}$, $\gamma = 1/(2a) + 1/(2b)$. No universal form for $G(q, \tau)$ is predicted, even if a stretched exponential is often observed [31].

The validity of MCT in describing the dynamics at the glass transition in a colloidal suspension of hard spheres was first proved by van Meegen and Pusey [34] by Dynamic Light Scattering experiments. Non-aqueous solutions of poly-methylmethacrylate particles stabilized against aggregation were concentrated and used to obtain metastable states capable of undergoing a glass transition at a critical concentration value. Further experiments on the same system inside the glass phase [35] confirmed that predictions of MCT correctly capture the dynamical features of the caging effect described by the β -relaxation. Some years later, Bergenholtz and Fuchs [36] pointed out that gelation of dilute solutions of colloidal particles interacting through strong, short range attraction, can be described in terms of the MCT picture. The main parameter is, in this case, the ratio between the particle size and the range of the attractive interaction, as the particle entrapment is due to the very high energy cost of liberating a caged particle.

RESULTS

On the sol side

By Static Light Scattering we measured the form factor of 0.2 % (w/w) HM pectin at T=20 °C in aqueous solution containing different amounts of sucrose (0-50%). A detailed data analysis has been reported in Ref. 28. Here we recall that the form factor, shown in Fig.1, is well described by the empirical expression found to be valid in the case of fractal clusters [37-38]:

$$P(q) = \left(1 + a (qR_g)\right)^{d_f/2} \quad \text{with} \quad a = \frac{2}{3d_f} \quad (7)$$

where d_f is the fractal dimension and R_g is the gyration radius in dilute solution. The expression also applies to the semidilute regime with R_g being a quantity proportional, with a factor of order one [39], to the static screening length. The latter represents the monomer-monomer correlation length beyond which excluded-volume interactions are screened by the presence of monomers of other chains [39-40]. We found $d_f = 1.55 \pm 0.1$. The dependence of R_g on sucrose concentration is shown in the inset of Fig. 1. The small, steady, increase of R_g is at odds with the expected reduction of solvent-exposed surface that sucrose should induce. Rather, the decrease of the solvent dielectric constant could be responsible for the increased chain stiffness through reinforcement of electrostatic interactions.

Changes in the sample dynamic properties were explored by Dynamic Light Scattering experiments. Electric field autocorrelation functions at different sucrose concentrations are plotted all together in Fig. 2. On increasing sucrose concentration from 0 to 50%, the main decay time increases by more than one order of magnitude, while the contribution of a faster decay becomes more visible. A simple exponential decay fit to data was found to be very poor even at 0% sucrose, where the fast initial decay is not clearly visible. As we'll see in the following, the fast decay becomes even more visible in gelled samples where it can be clearly ascribed to the presence of small clusters of sucrose molecules [41]. However, due to the small amplitude of the fast mode and the shortage of experimental points in this time scale, we decided to consider the slow mode only and fit data to a stretched exponential function:

$$g^{(1)}(\tau) = A \exp \left[- \left(\frac{t}{\tau} \right)^{-\beta} \right]$$

(8)

This expression is often used to describe the heterogeneous dynamics of disordered materials such polymeric melts or supercooled liquids close to the glass transition [31]. This dynamics is the result of a distribution of structural relaxation times, whose width is characterized by the value of β ($0 < \beta < 1$), with smaller values corresponding to wider distributions. We found a gradual decrease of β from 0.9 to 0.8 on changing sucrose concentration from 0 to 50%, indicating an increase of the dynamic heterogeneity.

The mean relaxation time, $\langle \tau \rangle$, is calculated by:

$$\langle \tau \rangle = \frac{\tau}{\beta} \Gamma(\beta^{-1}) \quad (9)$$

where Γ is the gamma function. Fig. 3 shows on a log-log scale the mean relaxation time vs. q at different sucrose concentrations. A similar q^n dependence at any sucrose concentration is found. The exponent $n=2.3$ indicates a dynamics with a main contribution from Brownian diffusion ($n=2$) together with vibrational motions ($n=3$) [40]. The inset of Fig. 3 shows the relaxation times relative to each solution, normalized by the respective bulk viscosity values. The latter were taken from the literature [32]. The collapsing of data to a single curve indicates that the slowing down of pectin dynamics is entirely due to the bulk viscosity increase.

The viscosity values of HM-pectin solutions were determined by rheological measurements. Fig. 4 shows the resulting viscosity vs. the sucrose concentration, as compared with the solvent viscosity at the same sucrose concentration. The comparison shows that the diverging behavior of the sample's viscosity cannot be totally ascribed to the solvent viscosity, since the pectin contribution is seen to increase with sucrose concentration. Finally, we note that no sign of shear thinning, as observed by other authors [42], is visible under our conditions probably due to the lower value of pectin concentration used.

From sol to gel

In studying the sol-gel transition in systems that form physical gels, the kinetic aspects deserve to be carefully considered, especially when the tuning effect of a given parameter has to be evaluated. Indeed, depending on the technique employed [43], it may be arduous to exactly define the sol-gel transition point or the attainment of a steady state. The latter may be practically never

gained in several physical gels as a further phase (aging) of minor rearrangements is often observed in several physical gel as a further phase (aging) of minor rearrangements is often observed. At 0.2% pectin concentration and 60 % sucrose, a gel forms in a few hours, while some days are necessary at 58 % sucrose. For the purpose of comparing samples at equivalent final stages of gelation kinetics, we used the classical method of the falling balls for determining when a self-supporting network was formed. Samples at different sucrose concentrations were prepared and kept in a thermostated bath at 20 °C to be periodically checked until they were found capable of sustaining the weight of a small steel ball. Although this empirical method probably overestimates the time necessary for the formation of a stable structure, it provides a convenient tool when dealing with very long kinetics. Table I reports the so estimated times at different sucrose concentrations.

Gelled samples

Static light scattering data from gelled samples with different amounts of sucrose were collected by ensemble averaging as a function of the q-vector. Results are shown on a log-log plot in Fig. 5. No differences were observed in the q-dependence of the different samples. The fractal dimension, given by the slope of $\log(I)$ vs. $\log(q)$, is almost constant with a value ranging between 1.5 and 1.6, practically the same as that obtained in liquid samples.

Ensemble-average correlation functions measured by DLS on gels with different sucrose content are shown in Fig. 6. Only the results for three samples are reported to prevent overcrowding of the figure. The high value of the non-decaying component indicates that the major fraction of the scattered light comes from species that do not relax over the experimental time scale. Two decays are also visible: the first one, occurring on a time scale of a few tens of microseconds, is well described by an exponential; the second one takes a much longer time and can be represented by a stretched exponential decay. To ascertain the kind of motion associated to the first decay, we looked at its q-dependence in the gel at 60% sucrose. A linear relationship between Γ and q^2 was observed as shown in Fig. 7. This assures that the motion corresponds to a free diffusion of small objects inside the gel matrix. The latter could be sucrose clusters, whose presence has been observed in aqueous solution even at very low sucrose concentration [41]. This hypothesis was tested by measurements on a sample with 60% sucrose prepared following the same protocol, but without pectin. Similar Γ values were obtained as shown in Fig. 7. The slope of Γ vs. q^2 gives a diffusion coefficient of 8.1×10^{-7} cm²/s. To estimate the hydrodynamic radius of the diffusing sucrose clusters, the value of the local viscosity needs to be known. Using the bulk viscosity gives an unphysical value of 0.4 Å, whereas that of pure water gives 2.6 nm.

Following the suggestion that a glass transition could be entered on increasing sucrose concentration, as indicated by the results on liquid samples, we attempted a data analysis in terms of MCT. Data relative to the correlation function tail were fit to Eq. 2 with g_{\pm} given by Eq. 4. In a first run all fit parameters were left free. The small spread in the values of the exponent a suggested that we repeat the fitting procedure by keeping it constant and equal to the fit average value of 0.345. MCT predicts $0 < a < 0.5$, and a value of 0.305 was found in the case of hard colloidal spheres [33]. Fig. 8 shows the correlation functions scaled according to the results of the fitting procedure. The quantity shown in the figure is $[f(\tau)-f_c]/k$ with the $k = [h(q)*c_d]*(\tau_{\beta})^a$. In this way, each correlation function was normalized by its own parameters (the baseline offset f_c , the amplitude of the β -relaxation $[h(q)*c_d]$, and the scaling time τ_{β}) so that a unique time dependence obeying the MCT prediction should be observed at large τ . The continuous line in the figure represents the master function $g_{\pm} = (\tau)^{-a}$ for the β -relaxation with $\tau_{\beta} = 1$. Upon scaling, the long-time tails of data related to different sucrose concentrations are made coincident over two orders of magnitude of time. This result confirms that, at least from a phenomenological point of view, MCT is applicable in our case, so indicating that the dynamic behavior is the same for each sample. For a quantitative comparison, the theoretical values of $f_c(q)$ and $h(q)$ need to be known, as calculated starting from an appropriate interaction potential. In its absence we can look at the dependence of the fit parameters on sucrose concentration. One prediction that can be easily tested is the dependence of τ_{β} on $|\sigma|^{1/2a}$. In panel A of Fig. 9, we plot $(1/\tau_{\beta})^{2a}$ vs. sucrose concentration to test the hypothesis that sucrose concentration plays the role of a critical parameter. The hypothesis appears reasonably valid. In panel B of the same figure the dependence of f_c and $[h(q)*c_d]$ are shown. The f_c behavior reflects the increasing degree of the freezing of the system with increasing sucrose concentration. No conclusions can be drawn from the decrease of the motional amplitude $[h(q)*c_d]$ with increasing sucrose concentration since the variation in $h(q)$ with changes in potential interaction at varying sucrose concentration is not known.

Mechanical properties of the gelled samples were characterized by measuring the viscoelastic spectra. Fig. 10 shows the dependence on frequency of the storage ($G'(\omega)$) and loss-modulus ($G''(\omega)$). The solid-like character of any sample is manifested by the nearly flat behavior of $G'(\omega)$, whose magnitude increases with the sucrose concentration. The viscous modulus $G''(\omega)$ increases quite linearly with ω over the entire frequency range and crosses $G'(\omega)$ at a frequency value that increases with increasing sucrose concentration. Except for the magnitude, no differences are seen in $G'(\omega)$ and $G''(\omega)$ behavior at varying sucrose concentration, thus suggesting that a master curve would be easily obtained. This was accomplished by firstly scaling $G'(\omega)$ and $G''(\omega)$ of each data set by the respective plateau modulus (A_G), and subsequently determining the scaling

factors (A_ω) for the frequency. The master curve shown in Fig. 11 is very similar to that observed for solidlike samples of weakly attractive colloidal particles above a critical value of particle concentration or interaction energy [44]. The relationship between the scaling factors is shown in the inset of Fig.11. The scaling of the viscoelastic data evidences that the increased solid-like character of gels with different sucrose contents is due to a higher extent of frozen structure formed by the same mechanism.

CONCLUSION

Tracing the mechanism of pectin gelation in the presence of sucrose to changes in the specific interactions between pectin, sucrose and water is made difficult by the lack of a clear understanding of the sugars effects on the gelation of biomolecules, as discussed in the Introduction. Here we have presented results on aqueous solutions of HM-pectin at varying sucrose concentrations, so as to span from liquid to gelled samples.

Pectin in sol samples appears as a system of branched clusters with strong hydrodynamic interactions. An increase in sucrose content induces a moderate increase in the screening length and a strong slowing down of the dynamics, proportional to the divergence in the bulk viscosity. The residue dynamics in gelled samples are seen to agree well with predictions of Mode Coupling Theory for the glass transition in supercooled liquids. This may appear quite surprising considering the complexity of the system under study, made of a natural polymer in sucrose-water solution. This finding further supports the idea that different phenomena characterized by an abrupt dynamic arrest can be described in a unified view [45]. In particular, it has been proposed that a jamming phase diagram, whose axes are density, interaction energy and applied stress, is capable of describing a wide variety of phenomena occurring in attractive colloidal systems such as the colloidal glass transition, gelation and aggregation [46]. This approach also provides useful indications of the relevant parameters for tailoring system properties. If the MCT model is used to describe the behavior of our system, sucrose concentration appears to play the role of a critical parameter for pectin gelation. Further work is necessary to determine whether the viscosity increase or the reinforcement of short range interactions, or both of these, are responsible for this effect.

ACKNOWLEDGEMENTS

We would like to thank Prof. J. Newman for his comments and a critical reading of the manuscript.

We also thank Dr. R. Noto for discussions and suggestions. Technical help from Mrs. F. Giambertone, G. Lapis and M. Lapis is also acknowledged.

REFERENCES

- 1) Mezzenga, R.; Schurtenberger, P.; Burbidge, A.; Michel, M. *Natures Materials* 2005, 4, 732-740.
- 2) van der Sman, R. G. M. ; van der Goot, A. J. *Soft Matter* 2009, 5. 601-510.
- 3) Willats, W.G.T.; Knox, J.P.; Mikkelsen, J.D. *Trends Food Sci. Tech.* 2006, 17, 97-104.
- 4) Grant, G. T.; Smith, P. J. C.; Thom, D. *FEBS Lett.* 1973, 32, 195-198.
- 5) Morris, V. J. In *Functional Properties of Food Macromolecules* Mitchell, J. R.; Ledward, D. A.; Eds.; (series name and number) Elsevier Applied Science Publishers: London, (UK) 1986; Chapter 3, p 121.
- 6) Rees, D. A. *Adv. Carbohydr. Chem. Biochem.* 1969, 24, 267-332.
- 7) Oakenfull, D.; Scott, A. *J. Food Sci.* 1984, 49, 1093-1098.
- 8) Somero, G. N. *Am. J. Physiol.* 1986, 251, R197-R213.
- 9) Timasheff, S. N. In *Water and Life*; Somero, G. N.; Osmond, C. B.; Bolis, C. L.; Eds.; Springer-Verlag: Berlin, 1990; Chapter 6, p 70-.
- 10) Arakawa, T.; Timasheff, S.N. *Biophys. J.* 1985, 47, 411.
- 11) Lee, J.C.; Timasheff, S.N. *J. Biol. Chem.* 1981, 256, 7193-7201.
- 12) Semenova, M.G.; Antipova, A.S.; Belyakova, L.E. *Curr. Opin. Colloid Interface Sci.* 2002, 7, 438-444.
- 13) Baierand, S.K.; McClements, D. J. *Comp. Rev. Food Sci. Food Safety* 2005, 4, 43-54.
- 14) Baier, S.; McClements, D.J. *J. Agric. Food Chem.* 2001, 49, 2600-2608
- 15) Dierckx, S.; Huyghebaert, A. *Food Hydrocolloids* 2002, 16, 489-497.
- 16) Kulmyrzaev, A.; Bryant, C.; McClements, D.J. *J. Agric. Food Chem.* 2000, 48, 1593-1597.
- 17) Kulmyrzaev, A.; Cancelliere, C.; McClements, D.J. *J. Sci, Food Agric.* 2000, 80, 1314-1318.
- 18) Evageliou, V.; Kasapis, S.; Hember, M. W. N. *Polymer* 1998, 39,3909–3917.
- 19) Nishinari, K.; Watase, M.; Miyoshi, E.; Takaya, T.; Oakenfull, D. *Food Technology* 1995, 49, 90–96.
- 20) Kasapis, S.; Al-Marhoobi, I.M.; Deszczynski, M.; Mitchell, J.R.; Abeyesekera, R. *Biomacromolecules* 2003, 4, 1142-1149.
- 21) Kasapis, S. *Food Hydrocolloids* 2001, 15, 631–641.
- 22) Nickerson, M.T.; Paulson, A.T.; Speers, R.A. *Food Hydrocolloids* 2004, 18, 783–794.

- 23) Al-Amri, I.S.; Al-Adavi, K.M.; Al-Marhoobi, I.M.; Kasapis, S. *Carbohydrate Polymers* 2005, *61*, 379–382.
- 24) Loret, C.; Ribelles, P.; Lundin, L. *Food Hydrocolloids* 2009, *23*, 823–832.
- 25) da Silva, J.A.L.; Gonçalves, M.P.; Rao, M.A. *Int. J. Biol. Macromol.* 1995, *17*, 25-32.
- 26) Al-Ruqaie, I.M.; Kasapis, S.; Richardson, R.K. *Polymer* 1997, *38*, 5685-5694.(pectina)
- 27) Kasapis, S.; Al-Alawi, A.; Guizani, N.; Khan A.J.; Mitchell, J.R. *Carbohydrate Polymers* 2000, *329*, 399-407 (pectina).
- 28) Bulone, D.; Martorana, V.; Xiao, C.; San Biagio, P.L. *Macromolecules* 2002, *35*, 8147-8151.
- 29) Bengtzelius, U.; Götze, W.; Sjölander, A. *J. Phys. C* 1984, *17*, 5915-...
- 30) Leutheusser, E. *Phys. Rev. A* 1984, *29*, 241-...
- 31) Götze, W.; Sjögren, L. *Rep. Prog. Phys.* 1992, *55*, 241-376.
- 32) Handbook of Chemistry and Physics; Weast, R. C., Astle, M. J., Beyer, W. H., Eds.; CRC Press: Boca Raton, FL, 1984; p D-265.
- 33) Pusey, P.; van Megen, W. *Physica A* 1989, *157*, 705-741.
- 34) van Megen, W.; Pusey, P.N. *Phys. Rev. A* 1991, *43*, 5429-5441.
- 35) van Megen, W.; Underwood, S. M. *Phys. Rev. E* 1994, *49*, 4206-4220.
- 36) Bergenholtz, J.; Fuchs, M. *Phys. Rev. E* 1999, *59*, 5706-5715.
- 37) Kallala, M.; Sanchez, C.; Cabane, B. *Phys. Rev. A* 1993, *48*, 3692-3704.
- 38) Trappe, V.; Bauer, J.; Weissmüller, M.; Burchard, W. *Macromolecules* 1997, *30*, 2365-2372.
- 39) Brown, W.; Nicolai, T. In *Dynamic Light Scattering*; Brown, W., Ed.; Clarendon Press: Oxford, 1993; Chapter 6, p 166.
- 40) Schaefer, D. W.; Han, C. C. In *Dynamic Light Scattering*; Pecora, R., Ed.; Plenum Press: New York, 1985; Chapter 5, p 181.
- 41) Kaufman, S.L.; Dorman, F. D. *Langmuir* 2008, *24*, 9979-9982.
- 42) Richter, S. *Macromol. Chem. Phys.* 2007, *208*, 1495–1502.
- 43) Sato, Y.; Kawabuchi, S.; Irimoto, Y, Miyawaki, O. *Food Hydrocolloids* 2004, *18*, 527-534.
- 44) Trappe, V.; Weitz, D.A. *Phys. Rev. Letters* 2000, *85*, 449-452.
- 45) Liu, A.J.; Nagel, S.R. *Nature* 1998, *396*, 21-22.
- 46) Trappe, V.; Prasad, V.; Cippelletti, L.; Segre, P.N.; Weitz, D.A. *Nature* 2001, *411*, 772-775.

FIGURE CAPTIONS

Fig.1 Form factor, $P(q)$, of 0.2% HM-pectin vs qR_g at different sucrose concentrations: 0% (black); 5% (red); 10% (green); 20% (blue); 30% (pink); 40% (cyan); 50% (orange). The continuous line is the fit to eq 1 in the text with $d_f=1.55$. The inset shows the R_g values at different sucrose concentrations.

Fig.2 Electric field auto-correlation functions $g^{(1)}(\tau)$ at 90° scattering angle for solutions of HM-pectin with different sucrose content. Color code as in Fig. 1.

Fig.3 Mean relaxation time, τ , vs q of HM-pectin in aqueous solution with different sucrose content on a log-log scale. In the inset τ -values were normalized for the solution bulk viscosity. Color code as in Fig.1.

Fig.4 Viscosity of aqueous solutions of HM-pectin with different sucrose content vs sucrose concentration (circles). The corresponding viscosity value of aqueous sucrose solution without pectin is also shown for comparison (triangles).

Fig. 5 Static light scattered intensity vs. q for gels of HM-pectin with different sucrose content: 55% (black); 56% (red), 57%(green), 58%(blue), 60%(pink); 62.5%(cyan), 65% (orange). The intensity values were obtained by averaging over different sample regions.

Fig.6 Ensemble average electric field auto-correlation function measured at 90° scattering angle on gels of HM-pectin with sucrose content of: 55% (empty circles), 58% (full circles), 60% (empty diamonds).

Fig.7 q -dependence of the relaxation time of the initial fast decay time for a gel of HM-pectin with 60% sucrose (black circles), and an aqueous solution with 60% sucrose (white triangles).

Fig.8 Ensemble-average electric field autocorrelation functions scaled according to Eq. 2. The critical parameters $f_c(q)$ and $[h(q)*c_\sigma]$ are given in Fig. 9. The solid line represents the master function $g_\pm(\tau)$ with $\tau_\beta=1$ for the β process of Mode Coupling theory.

Fig.9 Fit parameters to Eq. 2 of the correlation functions of gelled samples vs. sucrose concentration. Panel A: $(1/\tau_\beta)^{2a}$; panel B: f_c (full square); $[h(q) c_o]$ (empty triangles);

Fig.10 Mechanical spectra ($G'(\omega)$ (full symbols), $G''(\omega)$ (empty symbols)) measured on HM-pectin gels with different sucrose content: 56% (black); 58% (red), 60% (green); 62.5% (blue), 65% (pink).

Fig.11 Master curve showing the scaled moduli $G'_s(\omega)$ and $G''_s(\omega)$ vs. the scaled frequency ω_s . Color code as in Fig.10. The inset shows the relationship between the scaling factors.

TABLE I
Waiting time (t_w) for the formation of
a self-supporting structure

$C_{\text{Sucrose}} (\%w/w)$	t_w (hr)
55	320
56	150
57	72
58	35
60	6
62.5	1.5
65	0.5

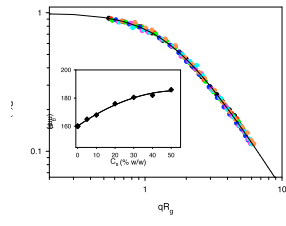


FIG. 1

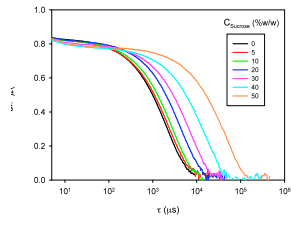


FIG. 2

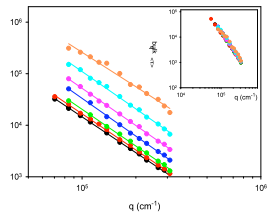


FIG. 3

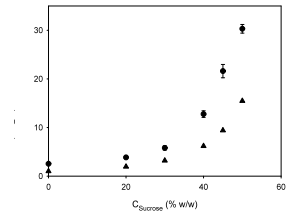


FIG. 4

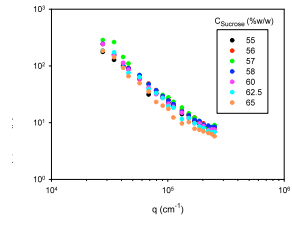


FIG. 5

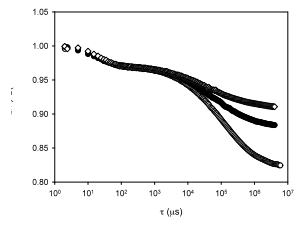


FIG. 6

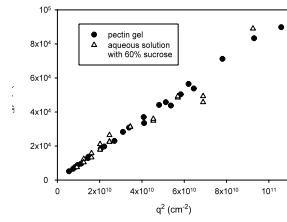


FIG. 7

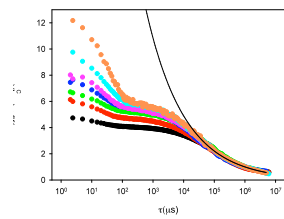


FIG. 8

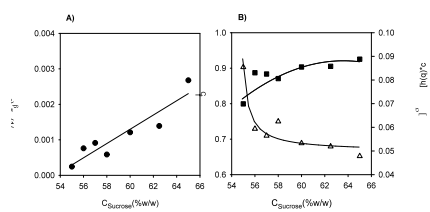


FIG. 9

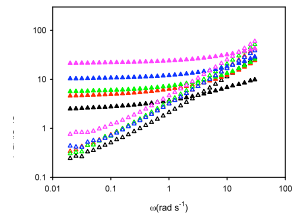


FIG. 10

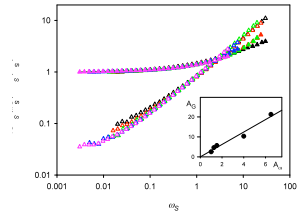


FIG. 11